Phosphonic acid-based membranes as proton conductors prepared by a pulsed plasma enhanced chemical vapor deposition technique

Arnaud Joël Kinfack Leoga, Loraine Youssef, Stéphanie Roualdes, V. Rouessac

Phosphonic acid-based membranes as proton conductors prepared by a pulsed plasma enhanced chemical vapor deposition technique

Arnaud Joël Kinfack Leoga, Loraine Youssef, Stéphanie Roualdès*, Vincent Rouessac

Institut Européen des Membranes (IEM), ENSCM, UM, CNRS UMR5635, Université de Montpellier, Place Eugène Bataillon, CC047, 34095 Montpellier, Cedex 5, France

Among the electrolyte membranes for proton conduction in hydrogen production systems and fuel cells, phos-phonic acid-based membranes are promising because of their advantage as good proton conductors in anhydrous medium which allows their use in systems operating at high temperature (80–150 °C) which is not the case of sulfonic acid-based ones such as the well-known Nafion® commercial membrane. In this study, a plasma poly-merization process using a continuous or pulsed glow discharge has been implemented to prepare original Plasma Enhanced Chemical Vapor Deposition (PECVD also called plasma polymerization) phosphonic acid-based membranes using dimethyl allylphosphonate as a single precursor. The structural and proton transport prop-erties of such membranes have been correlated with the plasma parameters in the deposition of films. The membranes prepared by pulsed plasma deposition method exhibit a better proton conductivity than that of membranes prepared by continuous plasma deposition method, in direct relation with their specific structural properties. The optimal plasma membrane, obtained in a pulsed 100 W plasma discharge, has shown specific resistance to proton conduction twice less than Nafion® 212 one which is great for the final applications of such membrane.

1. Introduction

In the current environmental context, alternative energy sources and the reduction of greenhouse gases become essential. One promising approach is the use of renewable energy, such as hydroelectric power, wind, solar and more recently hydrogen as clean, sustainable and non-polluting energy source [1,2] through its conversion in fuel cells. Polymer electrolyte membrane fuel cells (PEMFCs) are currently the most popular type of fuel cells. Their applications are multiple as much in the automotive field as in the stationary and portable domains. These systems operate with hydrogen (being the fuel with the highest energy capacity per unit mass) and oxygen and emit only water in the vapor form. Clean hydrogen can be generated from many processes notably by water electrolysis [3–5], electrocatalytic oxidation of formic acid [6] and electrocatalytic oxidation of ethanol [7]. The hydrogen production by water electrolysis is the most developed process, leading to high purity hydrogen [8]. Recently, the researchers have shown that the pure hydrogen production from water is not only possible by water electrolysis but also by water photo-electrolysis which is a very less energy consumer compared to water electrolysis. The photoassisted production of hydrogen and oxygen from water offers an extremely promising way for clean, low-cost and environmentally friendly conversion of solar into chemical energy.

The hydrogen production from water photo-electrolysis by solar light was first investigated in 1972 by Fujishima et al. [9]. The hy-drogen production system described in Fujishima study is based on a photo-catalytic activity of a titania layer used to split water into pro-tons, oxygen and electrons in the anodic compartment. Then protons are reduced in hydrogen H_2 on a solid cathode surface. Both electrodes are immersed in acidic liquid compartments separated by a ionic con-ductor medium. Since the innovative work of Fujishima, some other authors have been interested in photo-electrochemical systems for hy-drogen production, using solid catalytic photo-anode and cathode. These authors have sought to bring the solid electrodes and the ion exchange membrane together (integration strategy) to constitute a solid membrane/electrodes assembly (without any liquid solution) [10–13]. Nevertheless, neither of photo-electrochemical systems described in the literature is really integrated (that is to say based on a μ-architectured multilayers geometry) or involves plasma layers, as it is the case in our own approach.

Most of the hydrogen production systems and PEMFCs based on proton exchange membrane in the literature use perfluorinated com-mercial membranes notably Nafion® (by DuPont de Nemours) for proton transport. Several advantages of Nafion® have been

demonstrated such as excellent chemical, mechanical and thermal stabilities as well as high proton conductivity (60–100 mS·cm^{-1}) in the temperature range of 30–80 °C [14,15]. However, the dependence of Nafion® proton transport mechanism on water causes its poor conductivity at high operating temperature (above 80 °C) and then motivates the search to find a membrane which combines high proton conductivity and chemical, mechanical and thermal stabilities in the 80–150 °C range. Also, some other disadvantages of perfluorinated polymers are: fluorine chemistry requires drastic synthesis conditions to ensure safety and environmental protection and their use and recycling leads to the formation of corrosive, toxic compounds with a strong impact on the environment. Based on all disadvantages of perfluorinated membranes, phosphonic acid-based membranes seem to be very good candidates to replace perfluorinated membranes. Indeed, -PO$_3$H$_2$ groups in phosphonic acid-based membranes are amphoteric and possess a relatively high dielectric constant. The combination of these properties leads to a high degree of auto-dissociation which favors the formation of a hydrogen-bonding network making the proton conductivity independent of relative humidity and temperature, which allows the proton transport through an anhydrous conduction mechanism also known as the Grotthuss mechanism [16].

According to the literature, most of the phosphonic membranes are synthetized by conventional methods such as traditional polymerization of phosphonated monomers [17–20] or chemical grafting of phosphonic acid groups on unfunctionalized polymers [21,22]. Because of many disadvantages encountered with membranes obtained by conventional methods, plasma polymerization allows the manufacturing of dense, uniform and defect-free thin films on the substrate surfaces [23,24]. A previous study from our group has shown that the phosphonic acid-based membranes prepared by plasma polymerization were dense uniform and defect-free [25]. The highly cross-linked structure of plasma polymers leads to a low permeability of gases and organic liquids diffusion in the membrane [25,26] which are the main challenges in the yield drop of electrochemical systems.

Many researchers have investigated the plasma polymerization method [23–29]. Some researchers have highlighted the interest of pulsed plasma deposition method to generate chemically better defined plasma polymer films [24,27,28]. The pulsed radiofrequency (RF) plasma polymerization was first established by Yasuda et al. [29] in 1977. A. Ennajdaoui et al. [24] demonstrated that in a certain range of plasma conditions, a pulsed plasma discharge was better than a continuous plasma discharge enabling to deposit plasma polymers with better polymer structure and with higher deposition rate.

In the present study, we investigated both the continuous and pulsed deposition methods using dimethyl allylphosphonate as a single precursor. This work is based on a previous study by our group [25] which consisted in proving the feasibility to prepare phosphonic acid-based plasma-polymerized membranes using such a precursor. Only continuous plasma deposition method was investigated in this previous work.

The aim of this study is to investigate the influence of the plasma deposition conditions (continuous and pulsed) on the plasma polymers properties and to demonstrate the improving of the membrane properties by using of pulsed plasma deposition method. The physico-chemical and transport properties of prepared plasma membranes have been performed using different experimental methods. Morphology and thickness of plasma membranes were characterized by scanning electron microscopy (SEM). Their density was investigated by X-ray reflectometry (XRR). Chemical structure was determined using Fourier-transform infra-red spectroscopy (FTIR), energy dispersive X-ray spectroscopy (EDX) and X-ray photoelectron spectroscopy (XPS). Water sorption behavior of plasma membranes was investigated by ellipsometry coupled water sorption. Thermal stability was evaluated by thermogravimetric analysis (TGA). Lastly, functional properties as proton conductivity and specific resistance were measured by electrochemical impedance spectroscopy (EIS) using an environmental cell coupled to a potentiostat device.

2. Experimental section

2.1. Membrane preparation

The precursor used for the membrane preparation by plasma polymerization is the dimethyl allylphosphonate ([757-54-0], SP-61-001, supplied by SPECIFIC POLYMERS). This precursor, liquid at 20 °C, was put in a container under inert atmosphere of argon and heated at 70 °C. The precursor was transported in its gaseous state from the container to the reactor via a stainless steel pipe maintained at 80 °C, in order to avoid any recondensation. Argon (Air liquid, purity > 99.999%) was used as carrier gas. The gas mixture flow was controlled by a flowmeter (Bronkhorst EL-FLOW®).

All membranes were prepared in a 30 L lab-scale capacitively coupled plasma reactor [25] (MECA2000) pumped down by a primary pump (Adixen Pascal 2015 C1) associated with a turbomolecular pump (Alcatel Adixen ACT 200 T) for secondary pumping of the deposition chamber. Only the primary pump was used for the deposition process. The pressure inside the chamber was sensed and monitored by two gauges, a capacitive one (Leybold Vacuum Ceravak) for primary vacuum and a ionization one (Leybold Vacuum EV 25 QS AL) for secondary vacuum. A liquid nitrogen trap was positioned between the plasma chamber and the primary pump in order to trap the unreacted precursor and fragments vapors. A 13.56 MHz RF power source (Dressler CESAR 136) was used to supply power to the parallel and vertical plate disc electrodes (diameter: 10 cm, gap between electrodes: 2 cm). The grounded electrode could rotate (speed: 7 rad·s^{-1}).

Two types of substrate were used to support the plasma-polymerized films: silicon wafer (100) for structural characterizations (SEM, XRR, FTIR, EDX, XPS, ellipsometry and TGA) and E-Tek® support (20% porous carbon conductive fabric) supplied by De Nora® (previously called PEMEAS®) for functional characterizations (proton conductivity and specific resistance). This porous support is envisaged to be used in the final application (photo-electrolysis cell for hydrogen production by water splitting) as the gas diffusion layer in the cathodic compartment.

Before each deposition, silicon wafer was cleaned using acetone and ethanol baths. Then, substrates (silicon wafer and porous carbon conductive fabric) were both introduced into the deposition chamber which was maintained under low vacuum (at a limit pressure of 1×10^{-3} mbar) for few hours then under high vacuum (at a limit pressure of 1×10^{-5} mbar) for one hour in order to desorb all oxygen, water molecules and impurities adsorbed on the reactor walls. A 15 min long continuous plasma pre-treatment of supports was implemented before plasma polymerization using argon as gaseous phase (argon flow rate: 24 sccm and plasma discharge power: 100 W), in order to improve plasma film adherence.

During plasma polymerization, fixed deposition parameters were: the carrier argon flow rate equal to 4 sccm, the total pressure equal to 25×10^{-2} mbar and the deposition duration equal to 1 h. The two only variable plasma parameters during plasma polymerization were the plasma discharge power (60 W to 100 W) and the plasma deposition method (continuous or pulsed). The pulsed plasma deposition method consisted in performing the deposition by alternating T_{on} (time during which the plasma is on, equal to 5 ms) and T_{off} (time during which the plasma is off, equal to 5 ms). Pulse frequency was fixed at 100 Hz. So the duty cycle (DC), defined by Eq. (1) was equal to 0.5, i.e. 50%.

$$DC = \frac{T_{on}}{T_{on} + T_{off}} = T_{on} \times \text{pulse frequency} \tag{1}$$

After each deposition process (continuous or pulsed), the film obtained is composed of a cross-linked polymerized film covered by a condensation layer (formed of precursor and oligomers of it) as clearly identified in our previous study [25]. In order to polymerize this condensation layer, it was tried to apply a plasma post-treatment for
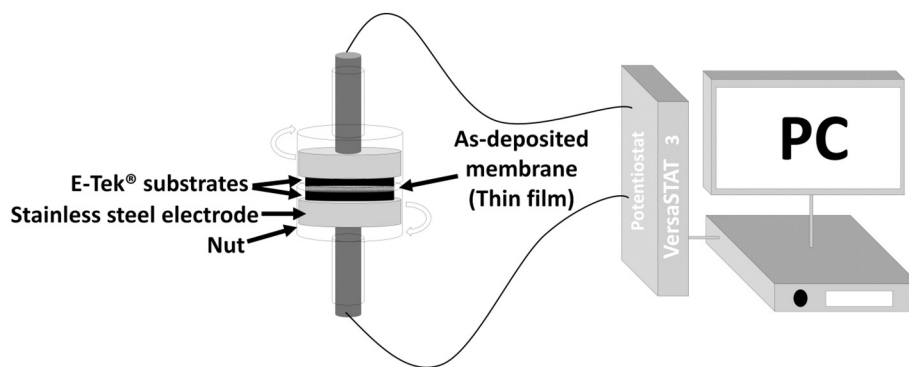
Fig. 1. Conductivity cell.

15 min using argon (flow rate: 24 sccm and plasma discharge power: 100 W). Despite this post-treatment, the condensation layer was still observed. So it was decided to abandon the post-treatment and to alternatively immerse all samples in ultra-pure water (Milli-Q® purification system, Millipore) after deposition in order to eliminate that unstable layer before each characterization, exactly as was applied in our previous study [25]. In this paper, all plasma films refer to post-washed materials and not to as-deposited materials.

2.2. Membrane characterization techniques

2.2.1. SEM analysis

The cross section and morphology of plasma polymers deposited on silicon wafer and porous carbon conductive fabric support were observed using scanning electron microscope (S-4800 Hitachi) to estimate the membranes thicknesses (error ~ 10%). For preparation to SEM analysis, plasma films deposited onto porous carbon conductive fabric supports were immersed in liquid nitrogen and broken in order to have a neat cut of the samples cross-section. Before each observation, the samples were Pt-metalized by sputtering under vacuum in order to make the surface electron conductive.

2.2.2. XRR analysis

XRR analysis was used to investigate the density of films deposited on silicon wafer by a Siemens/Bruker D5000 laboratory diffractometer (error 5%). The technique has been described in a previous article by our group [30].

2.2.3. FTIR, EDX and XPS analyses

The chemical composition of the plasma polymers deposited on silicon wafer was determined qualitatively by FTIR spectroscopy on a Nicolet 710 FTIR spectrometer (wavenumbers range: 4000–400 cm^{-1}; scans number per sample: 128; resolution: 4 cm^{-1}) and quantitatively by XPS on an ESCALAB 250 from Thermo Electron (monochromatic source of Aluminium 1486.6 eV; diameter of the analyzed surface: 400 μm) and by EDX with a scanning electron microscope (S-4500 Hitachi). The XPS analysis procedure is the same as that described in a previous paper by our group [31]. Before each EDX analysis, the samples were carbon-metalized with an ultra thin carbon layer in order to make the membranes electron conductor. EDX and XPS are complementary techniques; indeed the EDX analysis (covering a material volume of 1 $μm^3$) enables to investigate the bulk of films, whereas the XPS analysis (limited to an analysis depth of 10 nm) gives information on the surface composition. In both cases, the elemental (XPS and EDX) or environmental (XPS) atomic composition has a precision of 10 at.%.

2.2.4. Ellipsometry coupled with water sorption analysis

Ellipsometry analysis was used to evaluate the refractive index of plasma polymers, to verify the thickness locally measured by SEM and to investigate their behavior to water sorption by Semilab GES5E

Spectroscopic Ellipsometer (spectral range: 1.23–4.97 eV; Xenon lamp) completed with a lab-made set up for automatic adsorption-desorption with different intrusive vapor probes [32]. Water vapor has been used here as a probe. Before each water sorption analysis, the sample (film deposited on silicon wafer) was put under vacuum to desorb all water contained in the sample. A secondary vacuum was applied with a turbomolecular pump (Alcatel Drytel 1025). Then, ultra-pure water (Milli-Q® purification system, Millipore) was introduced progressively in the analysis chamber by monitoring the ratio P/P_0 with P being the water partial pressure and P_0 being the saturated vapor pressure of water at the analysis temperature. The thickness and refractive index at 633 nm of the plasma polymers were simultaneously calculated, using the optical model Cauchy law recorded every 60 s (corresponding to the stabilization time between each pressure level).

2.2.5. TGA analysis

A Thermogravimetric Hi-Res 2950 analyzer (TA Instruments) was employed to investigate the thermal stability behavior of plasma polymer films. About 97 mg of plasma polymer plus the substrate of silicon wafer were heated under nitrogen atmosphere up to 500 °C at a heating rate of 10 °C·min^{-1}.

2.2.6. EIS analysis

Prior to conductivity measurement, the membranes (plasma films onto porous carbon conductive fabric supports) were immersed in a 1 N H_2SO_4 solution for 24 h and afterwards rinsed with ultra-pure water (Milli-Q® purification system, Millipore) for 24 h, then, wiped to avoid having water on the membranes surfaces and then placed in the conductivity cell. The conductivity cell (Fig. 1) was a home-made cell constituted by two stainless steel electrodes clamping the plasma-polymerized membrane deposited on porous carbon conductive fabric support and another virgin porous carbon conductive fabric support, so that the plasma polymer was positioned between both porous carbon supports. Both external stainless steel electrodes could be tightened at a reproductible strength.

The proton conductivity $σ$ (mS·cm^{-1}) and specific resistance R_S (Ω·cm^2) of membranes were obtained from the film resistance R (Ω) determined from alternative current impedance analysis using a VersaSTAT 3 Potentiostat impedance analyzer, over the range of 10 μHz to 1 MHz with a controlled voltage. The film resistance R (Ω) was derived from the intersection of the high frequency semicircle on a complex impedance plane with the real Re (Z) axis. The proton conductivity $σ$ (mS·cm^{-1}) and specific resistance R_S (Ω·cm^2) were calculated using Eqs. (2) and (3):

$$σ \ (\text{mS·cm}^{-1}) \ = \ \frac{e}{R \ \times \ S} \tag{2}$$

$$R_S \ (\text{Ω·cm}^2) \ = \ R \ \times \ S \tag{3}$$

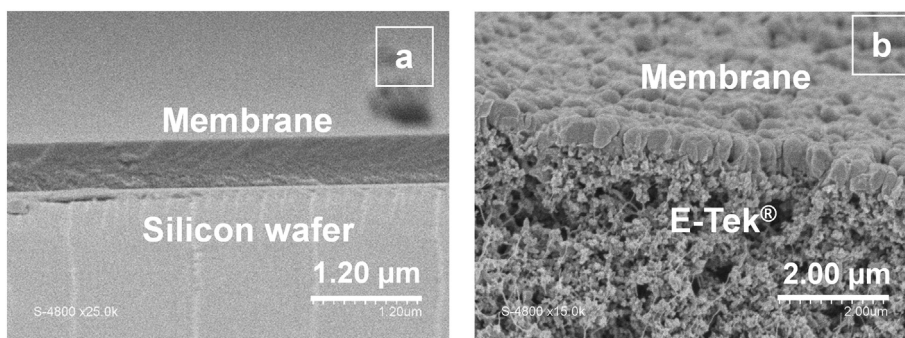where e is the membrane thickness, R the membrane resistance and S

Fig. 2. Membrane deposited at 60 W with pulsed plasma deposition method on (a) silicon wafer and (b) porous carbon conductive fabric support.

the active surface measurement (0.385 cm^2).

3. Results and discussions

3.1. Structural characterizations of plasma films

3.1.1. Morphology, growth rate and density measurement of plasma films

Whatever the kind of support silicon wafer or porous carbon conductive fabric, SEM pictures have shown that plasma polymers are dense, uniform, defect-free and very adherent on support. Fig. 2 shows a SEM cross-section view of a typical plasma membrane deposited on silicon wafer (Fig. 2-a) and on porous carbon conductive fabric (Fig. 2-b) for 1 h deposition time.

Fig. 3 shows the evolution of membrane growth rate on silicon wafer and E-Tek® support as a function of the plasma deposition conditions (continuous or pulsed). The growth rates are obtained from the membrane thicknesses measured by SEM analysis (error ~ 10%). The thicknesses of the films have been confirmed by ellipsometry. Similar highest growth rate (~17 nm.min^{-1}) and thickness (~1 µm) are obtained on both supports for the membrane deposited at 100 W with pulsed plasma deposition method. The aim of pulsed plasma deposition method is to less fragmentate the precursor in the gaseous phase in order to promote higher growth rate and lower cross-linking degree (generally enhancing proton transport). Concretely, it can be explained by the fact that more reactive species created during the T_{on} have higher probabilities to diffuse during the T_{off} and to react with the surface without any possible further fragmentation. This observation is in good agreement with the work of Retzko et al. [33] who found the deposition rates of plasma-polystyrene to be higher under pulsed plasma conditions than under continuous plasma conditions.

The density of the plasma films is an essential structural factor; indeed it defines the chain's crosslinking degree (ignoring the presence
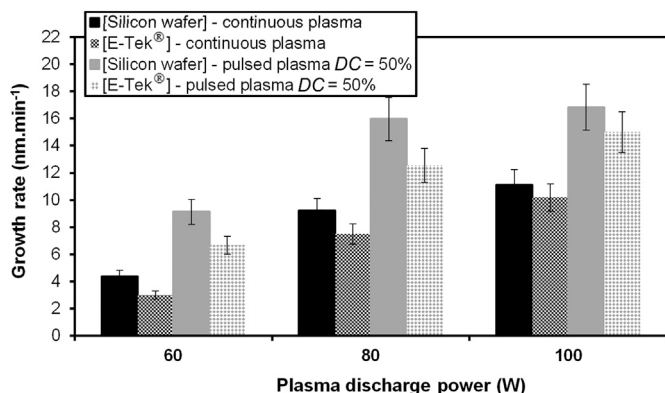

Fig. 3. Evolution of the film's growth rate deposited on silicon wafer or porous carbon conductive fabric support as a function of the plasma discharge power (ε ~ 10%).

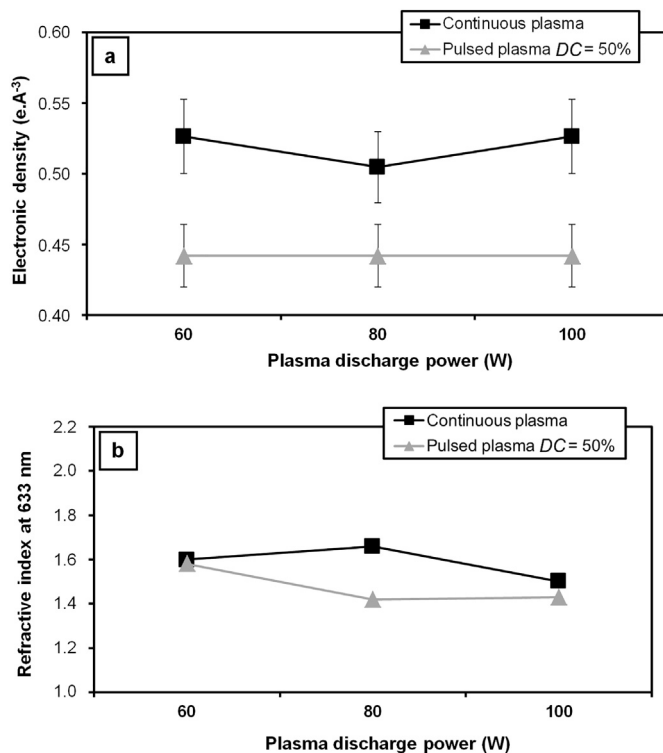**Fig. 4.** Evolution of the film's (a) density as a function of the plasma deposition conditions (ε ~ 5%) (b) refractive index as a function of the plasma deposition conditions.

of hydrogen in the films) which may have an important influence on the film's transport properties. The electronic densities of synthesized plasma films (Fig. 4-a), are comprised between 0.44 e·A^{-3} and 0.53 e·A^{-3} (error ~ 5%). These densities are 10 times less than the electronic density of gold (4.656 e·A^{-3}) but close to the electronic density of silicon (0.701 e·A^{-3}) measured by A. van der Lee et al. [34]. So plasma films prepared in this study are proved to be very dense. Moreover it can be noticed that all plasma films prepared with pulsed plasma deposition method are less dense than the ones prepared by continuous plasma deposition method. The lower density of plasma films prepared by pulsed plasma deposition method is directly related to softer fragmentation in the gaseous phase. Indeed, in pulsed discharge, the fragments are bigger (because the precursor globally undergoes less fragmentation) and when they recombine to form the deposit, they generate more free volume; consequently the overall network density is lower. The larger free volume in films deposited in pulsed plasma conditions should be a very good advantage in proton conduction, which will be investigated in part 3.2.

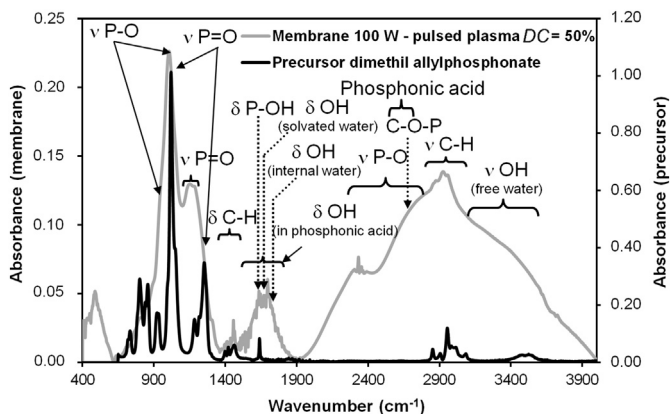The refractive indexes (at 633 nm) of plasma polymerized thin films

Fig. 5. FTIR spectra of the membrane deposited at 100 W with pulsed plasma deposition method (grey colour) and of the precursor dimethyl allyl phosphonate (black colour).
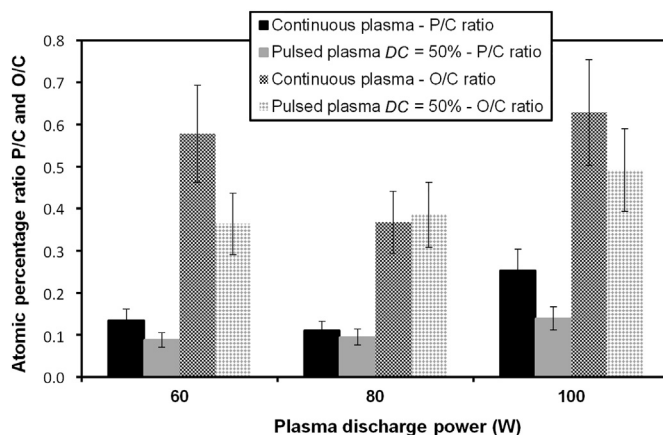

Fig. 6. Evolution of the film's atomic percentage ratio P/C and O/C as a function of the plasma deposition conditions obtained from atomic percentages measured by EDX ($\varepsilon \sim 20\%$).

(Fig. 4-b) are globally around 1.4–1.6 because of highly cross-linking degree of plasma polymers [35]. Plasma films prepared with continuous plasma conditions have higher refractive index than the ones prepared by pulsed plasma deposition method. This hierarchy is logical; indeed, higher densities (previously depicted by XRR for continuous conditions) generally lead to higher refractive indexes according to the Clausius-Mossotti relationship [36,37].

3.1.2. Chemical composition of plasma films

In order to qualitatively investigate the chemical structure of plasma polymers, FTIR analysis was performed. As an example of sample representative of the entire family of prepared plasma polymers, Fig. 5 shows the FTIR spectrum of the membrane deposited at 100 W with pulsed plasma deposition method (recorded with the transmission mode) in comparison to the FTIR spectrum of the precursor dimethyl allylphosphonate (recorded with the Attenuated Total Reflectance mode). It appears that some bonds present in the plasma polymer come directly from the structural units of the precursor and that some new types of bonds are formed during the plasma polymerization process. The prepared plasma polymers contain broad bands, i.e. overlapped, which are typical of plasma polymers being amorphous, highly cross-linked and made of a a wide variety of bond arrangements. Unfortunately, broad bands make peak assignments somewhat more difficult [38]. The peak assignments are presented in Table 1 [25]. It can be noticed that the prepared plasma-polymerized membranes are composed of a mixture of hydrocarbon and phosphonated groups and in particular phosphonic acid groups, due to the presence of the absorption bands relative to ν P-OH stretching vibration at 922 cm^{-1}, 1002 cm^{-1}, 2250–2800 cm^{-1} region and the absorption bands relative to ν P=O stretching vibration at 1011 cm^{-1} and 1100–1200 cm^{-1} region. The existence of pronounced absorption bands at

Table 1
FTIR peak assignments of the phosphonic acid-based plasma polymers.

Wavenumber (cm^{-1})	Assignment
922, 1002	ν P−O in P−O−H
1011, 1100–1200, 1250	ν P=O in phosphonic acid
1350–1500	δ (C−H)
1500–1800	δ O−H in phosphonic acid
1641	δ P−OH
1600–1650	δ OH (solvated water)
1720	δ OH (internal water)
2250–2800	ν P−O in P−O−H
2550–2700	Phosphonic acid
2679	C−O−P
2800–3100	ν C−H
3100–3600	ν OH (free water)

1600–1650 cm^{-1} and 3100–3600 cm^{-1} assigned respectively to ν O−H stretching and bending vibration (free water) proves high water content in plasma films which should be a great advantage for proton conduction, which will be investigated in part 3.2.

Fig. 6 presents the evolution of atomic percentages ratio of phosphorus atoms over carbon ones (P/C) and oxygen atoms over carbon ones (O/C) obtained from the atomic percentages of the three elements P, O, C measured by EDX. Besides O/C ratio of the membrane prepared at 80 W in pulsed plasma deposition method, all the other atomic percentages ratio P/C and O/C characteristic of films prepared in a pulsed discharge are smaller than those of the membranes prepared in a continuous discharge. That means films prepared with pulsed plasma deposition method contain less phosphonated groups or phosphonic acid groups than films prepared with continuous plasma deposition method. This could be explained by the fact that in pulsed plasma deposition method, the precursor containing hydrocarbon chains is less fragmented in the gaseous phase so that the polymer obtained after plasma polymerization contains longer hydrocarbon chains, and thus more carbon than the polymer prepared with continuous plasma deposition method. The consequence of plasma polymers containing more hydrocarbon chains is that the chains of the polymers are longer, which is in accordance with the lowest density previously depicted. In terms of influence of the plasma discharge power, the highest atomic percentages ratio P/C and O/C are obtained for the membranes deposited at 100 W plasma power. The lowest values globally observed for the films deposited at 80 W are difficult to justify.

The chemical analysis of plasma deposits was also investigated by XPS technique. Fig. 7 shows the photoelectron spectrum and typical decomposition of C1s, O1s and P2p photoelectron peaks of plasma film prepared at 100 W with pulsed plasma deposition method, qualitatively representative of all materials. Whatever the plasma deposition conditions, two different peaks appear for the carbon (C1s A and C1s B) and the oxygen (O1s A and O1s B) indicating the presence of two chemical environments of each element. Regarding the chemical environments of phosphorus, two different peaks (P2p3 A and P2p3 B) appear and a second P2p doublet (P2p1 A and P2p1B) is required to fit the data. The corresponding bond energies and assignments are given in Table 2.

The carbon chemical environment C1s A (at 284.8 eV) corresponding to C−C(−C) and C−H bonds is assigned to the hydrocarbon groups forming the backbone of plasma polymers with a higher percentage (42 at.%) compared to C1s B (at 286.7 eV) corresponding to C−O(−C), C-O(−P) and C−P bonds mostly presents in the precursor than in the plasma polymers (with only 7 at.%). The O=P and O=C bonds corresponding to O1s A (at 531.5 eV) oxygen chemical environment are less present in the film's composition with a percentage of 14 at.% compared to the O−P and O−C bonds corresponding to O1s
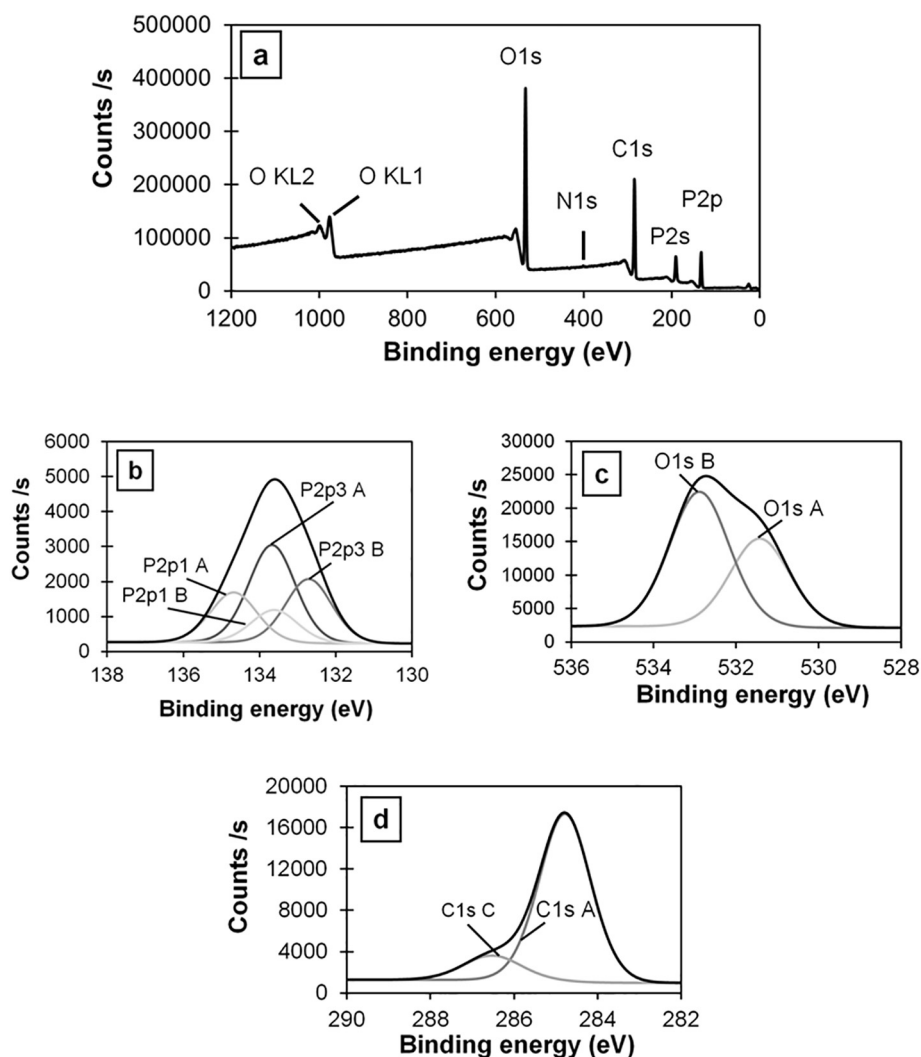
Fig. 7. XPS photoelectron spectrum (a) and XPS photoelectron peaks P2p (b), O1s (c) and C1s (d) of the plasma film prepared at 100 W with pulsed plasma deposition method.

Table 2
Bond energies and assignments of P2p, O1s and C1s XPS peaks characteristics of plasma films.

Photoelectron	Peak	Bonding energy (eV)	Assignment	References
P2p3	A	133.7 ± 0.1	P=O	[39,40]
	B	132.9 ± 0.1	P−C, P−O	[40,41]
O1s	A	531.5 ± 0.1	O=P, O=C	[40,42]
	B	532.9 ± 0.1	O−P, O−C	[40,42,43]
C1s	A	284.8 ± 0.1	C-C(−C), C−H	[41,42,44]
	C	286.7 ± 0.1	C−O(−C), C-O(−P), C−P	[41,42,45]

B (at 532.9 eV) which are 22 at.%.

Fig. 8-a shows the evolution of the film's atomic percentage of the phosphorus chemical environments as a function of the plasma deposition conditions. P2p3 A (at 133.7 eV) corresponding to P=O bonds are much higher in all the plasma films compared to P2p3 B (at 132.9 eV) corresponding to P−C and P−O bonds. Moreover the percentages of P2p3 B corresponding to P−C and P−O bonds responsible for proton conduction are quite similar in all the plasma films. All of that reveals the presence of phosphonated groups and phosphonic acid groups in plasma polymers, as previously observed by FTIR analysis.

The histogram showing the evolutions of the atomic percentages

ratio P/C and O/C obtained from the atomic percentages measured by XPS as a function of the plasma deposition conditions is presented in Fig. 8-b. These evolutions are qualitatively the same as the evolutions obtained by EDX, but quantitative comparison makes appear slightly higher values for XPS analysis. This quantitative difference proves that the surface of materials is a little bit more charged in P and O elements compared to the bulk of films. This attests that XPS and EDX are two complementary techniques.

3.1.3. Refractive index and swelling rate change following water sorption of plasma films

Plasma films have been characterized in terms of water sorption behavior. According to the refractive index of the water adsorption/desorption isotherms (not shown here), all the plasma films have been determined as non-porous films except the one prepared at 80 W with pulsed plasma deposition method which has shown a refractive index profile typical of a mesoporous material (isotherm of type IV according to the International Union of Pure and Applied Chemistry classification). The refractive index change and the thickness change as a function of the water partial pressure P/P_0 of the plasma film prepared at 100 W with pulsed plasma deposition method (as representative sample) is given in Fig. 9. As P/P_0 increases, the refractive index decreases from 1.64 down to 1.59 while the film thickness rises from 800 nm to 980 nm. By making the hypothesis that the refractive index
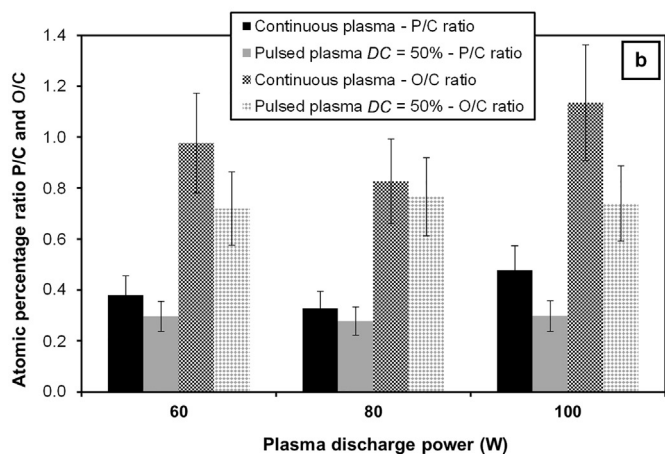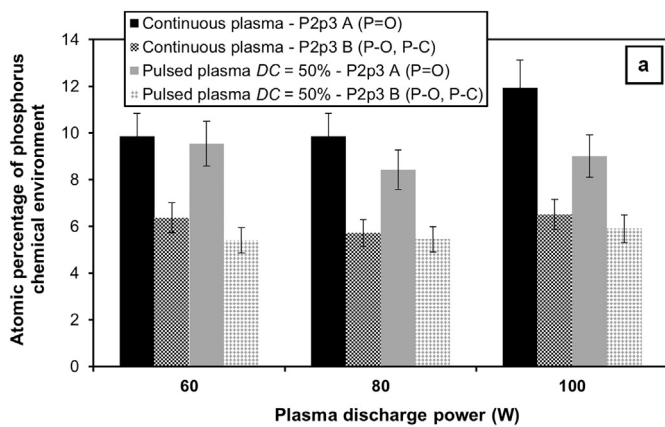
Fig. 8. Evolution of the film's atomic percentage (a) of the phosphorus chemical environments ($\varepsilon \sim 10\%$) and (b) ratio P/C and O/C ($\varepsilon \sim 20\%$) obtained from the atomic percentages obtained from XPS analysis as a function of the plasma deposition conditions.
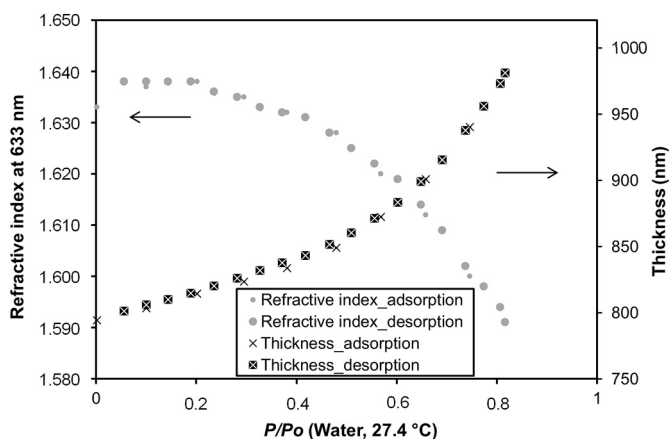

Fig. 9. Refractive index change (grey colour) and thickness change (black colour) following water sorption of the plasma film prepared at 100 W with pulsed plasma deposition method.

of the film absorbing water molecules in its network is a combination of the refractive index of the dry material (1.64) and the refractive index of the liquid water phasis (1.33), an explanation of the refractive index decrease when the water pressure increases is that water progressively replace the free volume, and then infiltrates between the polymer chains, dilating them. Thus, the global dielectric constant, i.e. the refractive index, is decreasing.

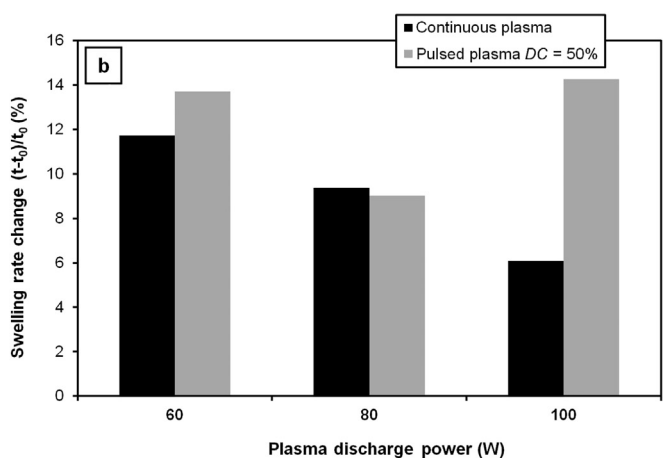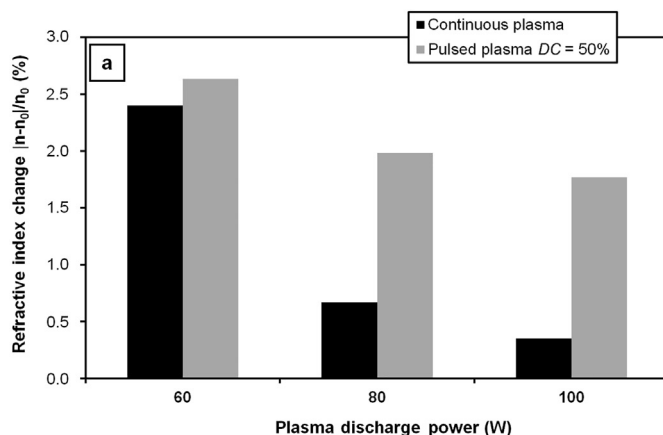Fig. 10 shows the evolution of the absolute value of the refractive

Fig. 10. Evolution of (a) the absolute value of the refractive index change $|n-n_0|/n_0$ (%) and (b) the swelling rate change $(t-t_0)/t_0$ (%) following water sorption of the plasma films.

index change and the swelling rate change due to water sorption of the plasma films obtained at the water partial pressure of $P/P_0 = 0.7$. Excepted the film prepared at 80 W with pulsed plasma deposition method (Fig. 10-b), a general tendance is that refractive index and swelling rate changes are higher for the membranes prepared with pulsed plasma deposition method than for the membranes prepared with continuous plasma deposition method, probably because they are less dense and they have more flexible chains, enabling more pronounced variation of free volume. This has been also shown by Nicole Timmerhuis et al. [46] for water-toluene mixtures penetration in polysulfone films. According to S. C. Pathak et al. [35] works, the variation of refractive index and swelling rate change of thin films in aqueous environments are directly related to crosslink density of the films. The higher refractive index change of the membranes prepared by pulsed plasma deposition method can be directly related to their higher water uptake capacity which could be a very good advantage in proton conduction, which will be investigated in part 3.2.

3.1.4. Thermal stability investigation of plasma films

The thermogram of the plasma film prepared at 100 W with pulsed plasma deposition method (Fig. 11) is only qualitatively exploitable as the weight loss is very low due to the fact that the analysis was performed on a sample composed of the plasma polymer deposited on its silicon substrate. However three main weight losses can be depicted. The first weight loss between 100 °C and 250 °C, typically assigned to the desorption of free and adsorbed water, is quite absent in the thermogram, which proves that phosphonic acid-based plasma membranes either contain very few water or retain water very well even at
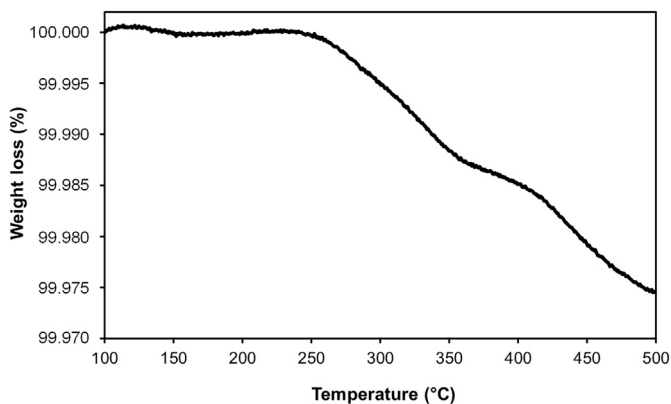
Fig. 11. Thermogram of the plasma film prepared at 100 W with pulsed plasma deposition method.

temperature as high as 250 °C [47,48]. The second weight loss between 250 °C and 350 °C can be attributed to the defragmentation of ether groups and the cleavage of the P—C bonds in the polymer matrix [49]. The third weight loss observed from 350 °C until 490 °C may arise from self-condensation reactions, which form anhydride bonds between the phosphonic groups [50]. All other plasma films show quite the same thermogram which allows us to say that, all plasma phosphonic membranes present a good thermal stability up to 250 °C in terms of both water management and covalent network.

3.2. Functional charaterizations of plasma films

In order to functionally characterize the membranes, proton conductivity and specific resistance were measured by EIS. Fig. 12-a shows the evolution of the film's proton conductivity as a function of the plasma deposition conditions at the temperature of 25 °C and 100% relative humidity (RH). As expected considering structural properties previously investigated, all plasma films prepared by pulsed plasma deposition method show proton conductivity higher than the films prepared by continuous plasma deposition method. The best conductivity ($\sigma = 0.14$ mS·cm^{-1}) has been obtained for the membrane prepared at 100 W with pulsed plasma deposition method. Table 3 presents the thickness, the proton conductivity and the specific resistance measured in the same cell for the membranes prepared at 100 W plasma powers (continuous and pulsed) and for the Nafion® 212. When compared to the Nafion® 212 ($\sigma = 6.70$ mS·cm^{-1}; $Rs = 1.52$ Ω·cm^2), the best plasma polymer is 40 times intrinsically less conductive than the Nafion® 212 commercial membrane because of high cross-linked degree inherent to plasma polymers. But, the best plasma membrane is extensively very competitive due to its specific resistance being three times less than the Nafion® 212 due to its low thickness. As a remark, it can be mentioned that conductivity values measured with our cell are lower (factor 10) than some measured with other cells in the literature (for Nafion® 212: $\sigma = 60$ mS·cm^{-1} at 25 °C and 95% RH by Lin et al. [51] as an example) probably due to poor contact between stainless steel electrodes and membrane.

Fig. 12-b shows the evolution of the film's proton conductivity as a function of the temperature and RH for the different plasma deposition conditions. The conductivity of the membrane deposited at 60 W with continuous plasma deposition method is in the same order than the one prepared by J. Bassil et al. [25] ($\sigma = 0.08$ mS·cm^{-1} at 20 °C and 90% RH) in a previous study by our group. It can be observed that, whatever the measurement conditions, all the films prepared with pulsed plasma deposition method have higher conductivities than the films prepared with continuous plasma conditions. These evolutions have the same trend as the evolutions obtained with the conductivities measured at 25 °C and 100% RH. The conductivities of the films decrease not so much by decreasing the relative humidity from 90% to 30% (by
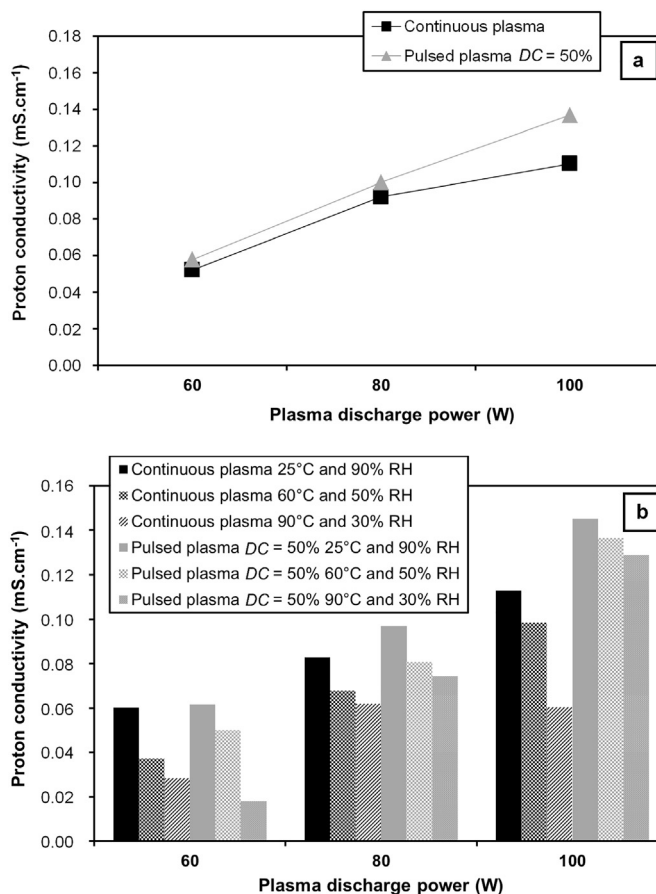

Fig. 12. Evolution of the film's proton conductivity (a) measured at 25 °C and 100% RH and (b) measured at different temperatures 25–90 °C and RH 30–90% as a function of the plasma deposition conditions.

Table 3
Thickness and proton transport properties of the plasma films prepared at 100 W plasma powers and of the Nafion® 212 commercial membrane.

Membrane	Thickness (µm)	Proton conductivity σ (mS·cm^{-1})	Specific resistance Rs (Ω·cm^2)
Nafion® 212	50	6.70	1.52
Membrane 100 W – pulsed plasma DC = 50%	1	0.14	0.66
Membrane 100 W – continuous plasma	0.65	0.11	0.55

simultaneously increasing the temperature from 25 °C to 90 °C) which proves that the proton conductivity of phosphonic acid-based membranes are not so dependent of the relative humidity and the temperature that allows their proton transport even in anhydrous medium. At 90 °C and 30% RH (which are close conditions to those of the real fuel cell), the best film is the membrane prepared at 100 W with pulsed plasma deposition method with a conductivity equal to $\sigma = 0.13$ mS·cm^{-1} two times more than the conductivity of the equivalent membrane prepared with continuous plasma conditions.

4. Conclusion

Competitive phosphonic acid-based membranes have been prepared by Plasma Enhanced Chemical Vapor Deposition (PECVD) process using dimethyl allylphosphonate as a single precursor in a RF PECVD reactor by using a mixture of argon and precursor in the gaseous phase. The

innovation in this study is that not only the continuous plasma deposition method but also the pulsed one have been investigated.

Whatever the plasma conditions may be, the prepared membranes show a high cross-linking degree (as shown by SEM and RRX), which should give them good impermeability to gases and organic liquids (as demonstrated in a previous work by our group [25]). Moreover, they are uniform, defect-free and very adherent on supports making expect good integration in multi-layered systems. Furthermore, they are stable in terms of water retain and covalent network up to 250 °C (as shown by TGA). All these properties should ensure high performance of hydrogen production systems including such electrolyte membrane (ideally operating at temperature up to 80–150 °C).

In terms of structural and functional properties, phosphonic acid-based membranes prepared with the pulsed plasma deposition method are more competitive than the membranes prepared under continuous plasma conditions. The optimal membrane has been prepared at 100 W with the pulsed plasma deposition method; its main characteristics are: thickness $\sim 1\,\mu m$, electronic density $0.53\,e\cdot A^{-3}$, proton conductivity and specific resistance respectively equal to $\sigma = 0.14\,mS\cdot cm^{-1}$ and $R_s = 0.66\,\Omega\cdot cm^2$ at 20 °C and 90% RH.

As prospects, such optimal membrane will be more deeply characterized in terms of water management (water diffusion measurements in progress) and will be integrated in an all-plasma photo-electrolysis cell, including an innovating TiO_2 photo-anode also developed in our research group [52], for hydrogen production by water splitting.

Acknowledgments

References

[1] P. Costamagna, S. Srinivasan, Quantum jumps in the PEMFC science and technology from the 1960s to the year 2000: part I. Fundamental scientific aspects, J. Power Sources 102 (2001) 242–252.

[2] K.D. Kreuer, On the development of proton conducting polymer membranes for hydrogen and methanol fuel cells, J. Membr. Sci. 185 (2001) 29–39.

[3] A.T. Marshall, S. Sunde, M. Tsypkin, R. Tunold, Performance of a PEM water electrolysis cell using $Ir_xRu_yTa_zO_2$ electrocatalysts for the oxygen evolution electrode, Int. J. Hydrog. Energy 32 (2007) 2320–2324.

[4] A. Marshall, B. Børresen, G. Hagen, M. Tsypkin, R. Tunold, Hydrogen production by advanced proton exchange membrane (PEM) water electrolysers—reduced energy consumption by improved electrocatalysis, Energy 32 (2007) 431–436.

[5] F. Barbir, PEM electrolysis for production of hydrogen from renewable energy sources, Sol. Energy 78 (2005) 661–669.

[6] C. Lamy, A. Devadas, M. Simoes, C. Coutanceau, Clean hydrogen generation through the electrocatalytic oxidation of formic acid in a Proton Exchange Membrane Electrolysis Cell (PEMEC), Electrochim. Acta 60 (2012) 112–120.

[7] C. Lamy, From hydrogen production by water electrolysis to its utilization in a PEM fuel cell or in a SO fuel cell: some considerations on the energy efficiencies, Int. J. Hydrog. Energy 41 (2016) 15415–15425.

[8] S.A. Grigoriev, V.I. Porembsky, V.N. Fateev, Pure hydrogen production by PEM electrolysis for hydrogen energy, Int. J. Hydrog. Energy 31 (2006) 171–175.

[9] A. Fujishima, K. Honda, Electrochemical photolysis of water at a semiconductor electrode, Nature 238 (1972) 37.

[10] K. Fujihara, T. Ohno, M. Matsumura, Splitting of water by electrochemical combination of two photocatalytic reactions on TiO_2 particles, J. Chem. Soc. Faraday Trans. 94 (1998) 3705–3709.

[11] E. Selli, G.L. Chiarello, E. Quartarone, P. Mustarelli, I. Rossetti, L. Forni, A photocatalytic water splitting device for separate hydrogen and oxygen evolution, Chem. Commun. (2007) 5022–5024.

[12] R. Tode, A. Ebrahimi, S. Fukumoto, K. Iyatani, M. Takeuchi, M. Matsuoka, C.H. Lee, C.-S. Jiang, M. Anpo, Photocatalytic decomposition of water on double-layered visible light-responsive TiO_2 thin films prepared by a magnetron sputtering deposition method, Catal. Lett. 135 (2010) 10–15.

[13] K.O. Iwu, A. Galeckas, A.Y. Kuznetsov, T. Norby, Solid-state photoelectrochemical H_2 generation with gaseous reactants, Electrochim. Acta 97 (2013) 320–325.

[14] T.A. Zawodzinski, C. Derouin, S. Radzinski, R.J. Sherman, V.T. Smith, T.E. Springer, S. Gottesfeld, Water uptake by and transport through Nafion® 117 membranes, J. Electrochem. Soc. 140 (1993) 1041–1047.

[15] S.R. Samms, S. Wasmus, R.F. Savinell, Thermal stability of Nafion® in simulated fuel cell environments, J. Electrochem. Soc. 143 (1996) 1498–1504.

[16] N. Agmon, The Grotthuss mechanism, Chem. Phys. Lett. 244 (1995) 456–462.

[17] T. Sata, T. Yoshida, K. Matsusaki, Transport properties of phosphonic acid and sulfonic acid cation exchange membranes, J. Membr. Sci. 120 (1996) 101–110.

[18] S.V. Kotov, S.D. Pedersen, W. Qiu, Z.-M. Qiu, D.J. Burton, Preparation of perfluorocarbon polymers containing phosphonic acid groups, J. Fluor. Chem. 82 (1997) 13–19.

[19] M. Yamabe, K. Akiyama, Y. Akatsuka, M. Kato, Novel phosphonated perfluorocarbon polymers, Eur. Polym. J. 36 (2000) 1035–1041.

[20] M. Yamada, I. Honma, Anhydrous proton conducting polymer electrolytes based on poly(vinylphosphonic acid)-heterocycle composite material, Polymer 46 (2005) 2986–2992.

[21] H.R. Allcock, M.A. Hofmann, C.M. Ambler, S.N. Lvov, X.Y. Zhou, E. Chalkova, J. Weston, Phenyl phosphonic acid functionalized poly[aryloxyphosphazenes] as proton-conducting membranes for direct methanol fuel cells, J. Membr. Sci. 201 (2002) 47–54.

[22] G. Schmidt-Naake, M. Böhme, A. Cabrera, Synthesis of proton exchange membranes with pendent phosphonic acid groups by irradiation grafting of VBC, Chemical Engineering & Technology 28 (2005) 720–724.

[23] A. Ennajdaoui, S. Roualdes, P. Brault, J. Durand, Membranes produced by plasma enhanced chemical vapor deposition technique for low temperature fuel cell applications, J. Power Sources 195 (2010) 232–238.

[24] A. Ennajdaoui, J. Larrieu, S. Roualdes, J. Durand, PECVD process for the preparation of proton conducting membranes for micro fuel cells. Impedance probe measurements and material characterizations, Eur. Phys. J. Appl. Phys. 42 (2008) 9–15.

[25] J. Bassil, S. Roualdès, V. Flaud, J. Durand, Plasma-polymerized phosphonic acid-based membranes for fuel cell, J. Membr. Sci. 461 (2014) 1–9.

[26] S. Roualdes, I. Topala, H. Mahdjoub, V. Rouessac, P. Sistat, J. Durand, Sulfonated polystyrene-type plasma-polymerized membranes for miniature direct methanol fuel cells, J. Power Sources 158 (2006) 1270–1281.

[27] T. Barman, A.R. Pal, J. Chutia, Comparative study of structural and optical properties of pulsed and RF plasma polymerized aniline films, Appl. Surf. Sci. 313 (2014) 286–292.

[28] Z. Jiang, Z.-j. Jiang, Synthesis and optimization of proton exchange membranes by a pulsed plasma enhanced chemical vapor deposition technique, Int. J. Hydrog. Energy 37 (2012) 11276–11289.

[29] H. Yasuda, T. Hsu, Some aspects of plasma polymerization investigated by pulsed R.F. discharge, Journal of Polymer Science: Polymer Chemistry Edition 15 (1977) 81–97.

[30] M. Schieda, F. Salah, S. Roualdès, A. van der Lee, E. Beche, J. Durand, X-ray reflectometry characterization of plasma polymer films synthesized from triallylamine: density and swelling in water, Plasma Process. Polym. 10 (2013) 517–525.

[31] M. Reinholdt, A. Ilie, S. Roualdès, J. Frugier, M. Schieda, C. Coutanceau, S. Martemianov, V. Flaud, E. Beche, J. Durand, Plasma membranes modified by plasma treatment or deposition as solid electrolytes for potential application in solid alkaline fuel cells, Membranes 2 (2012) 529–552.

[32] V. Rouessac, Porosimétrie de couches minces par ellipsométrie et microbalance à quartz, Institut Européen des Membranes, Atelier AMC, 2012.

[33] I. Retzko, J.F. Friedrich, A. Lippitz, W.E.S. Unger, Chemical analysis of plasma-polymerized films: the application of X-ray photoelectron spectroscopy (XPS), X-ray absorption spectroscopy (NEXAFS) and fourier transform infrared spectroscopy (FTIR), J. Electron Spectrosc. Relat. Phenom. 121 (2001) 111–129.

[34] A. van der Lee, Analyse structurale de couches minces par réflectométrie de rayons-X, Institut Européen des Membranes Montpellier, 2012.

[35] S.C. Pathak, D.W. Hess, Dissolution and swelling behaviour of plasma-polymerized polyethylene glycol-like hydrogel films for use as drug delivery reservoirs, ECS Trans. 6 (2008) 1–12.

[36] V. Cech, S. Lichovnikova, R. Trivedi, V. Perina, J. Zemek, P. Mikulik, O. Caha, Plasma polymer films of tetravinylsilane modified by UV irradiation, Surf. Coat. Technol. 205 (2010) S177–S181.

[37] H.G. Tompkins, Handbook of Ellipsometry, William Andrew/Springer, Norwich, 2005.

[38] R. D'Agostino, Plasma Deposition, Treatment and Etching of Polymers, Academic Press, Boston, USA, 1990.

[39] M.H. Basha, N.O. Gopal, D.B. Nimbalkar, S.-C. Ke, Phosphorus and boron codoping into TiO_2 nanoparticles, an avenue for enhancing the visible light photocatalytic activity, J. Mater. Sci. Mater. Electron. 28 (2017) 987–993.

[40] C. Viornery, Y. Chevolot, D. Léonard, B.-O. Aronsson, P. Péchy, H.J. Mathieu, P. Descouts, M. Grätzel, Surface modification of titanium with phosphonic acid to improve bone bonding: characterization by XPS and ToF-SIMS, Langmuir 18 (2002) 2582–2589.

[41] M. Wagstaffe, A.G. Thomas, M.J. Jackman, M. Torres-Molina, K.L. Syres, K. Handrup, An experimental investigation of the adsorption of a phosphonic acid on the Anatase $TiO_2(101)$ surface, J. Phys. Chem. C 120 (2016) 1693–1700.

[42] P.R. Davies, N.G. Newton, The chemisorption of organophosphorus compounds at an Al(111) surface, Appl. Surf. Sci. 181 (2001) 296–306.

[43] D. Briggs, M.P. Seah, Practical Surface Analysis: Auger and X-ray Photoelectron Spectroscopy, 2nd ed., John Wiley & Sons, Chichester, UK, 1990.

[44] L.J. Gerenser, An x-ray photoemission spectroscopy study of chemical interactions at silver/plasma modified polyethylene interfaces: correlations with adhesion, J. Vac. Sci. Technol. A 6 (1988) 2897–2903.

[45] C.H. Liu, C. Huang, Structural changes of boron carbide induced by Zr incorporation, J. Mater. Sci. 35 (2000) 387–390.

[46] N. Timmerhuis, Bachelor assignment Inorganic Membranes, Universiteit Twente, July 2015.

[47] L. Woźniak, J. Chojnowski, Silyl esters of phosphorous—common intermediates in

synthesis, Tetrahedron 45 (1989) 2465–2524.

[48] K. Afarinkia, C.W. Rees, J.I.G. Cadogan, Synthesis of organophosphorus compounds via silyl esters of phosphorous acids, Tetrahedron 46 (1990) 7175–7196.

[49] J. Parvole, P. Jannasch, Poly(arylene ether sulfone)s with phosphonic acid and bis (phosphonic acid) on short alkyl side chains for proton-exchange membranes, J. Mater. Chem. 18 (2008) 5547–5556.

[50] D.D. Jiang, Q. Yao, M.A. McKinney, C.A. Wilkie, TGA/FTIR studies on the thermal degradation of some polymeric sulfonic and phosphonic acids and their sodium salts, Polym. Degrad. Stab. 63 (1999) 423–434.

[51] J. Lin, P.-H. Wu, R. Wycisk, P. Pintauro, PEM fuel cell properties of pre-stretched recast Nafion®, ECS Trans. 16 (2008) 1195–1204.

[52] L. Youssef, A.J. Kinfack Leoga, S. Roualdes, J. Bassil, M. Zakhour, V. Rouessac, A. Ayral, M. Nakhl, Optimization of N-doped TiO_2 multifunctional thin layers by low frequency PECVD process, J. Eur. Ceram. Soc. 37 (2017) 5289–5303.